FREDERICK S. BILLIG

TACTICAL MISSILE DESIGN CONCEPTS

The selection of a propulsion system to meet a particular mission requirement is arduous and often controversial. Frequently, when the government solicits proposals for missile concepts from industry, it must choose from a group of fundamentally different propulsion concepts. This article describes a variety of propulsion cycles and presents a methodology for selection based on particular mission requirements and constraints. Engine specific impulse, thrust-to-weight ratio, and propellant mass fraction are shown to be important engine design indices that govern selection. Optimal staging, motor pulsing, and thrust modulation are among the design variables that are examined.

INTRODUCTION

From the Wright Flyer to the Space Shuttle, propulsion has set the pace for the technology of flight. At first it seemed to present an insurmountable barrier, but once overcome by the development of a variety of efficient power plants, new vistas of opportunity have presented themselves.

Tactical missile development was no exception. Initially, the challenge was to produce enough thrust to reach and sustain a velocity with a payload of sufficient size for a viable weapon concept. Later the goal was to produce a thrust greater than the weight of the missile and sufficient to penetrate the so-called "sonic barrier." That challenge was met by the rocket, the subsonic combustion ramjet, the turbojet, and other engine cycles. Currently we seek to fly at hypersonic speeds (greater than five times the speed of sound) to long ranges within the lower atmosphere. Perhaps this will be accomplished when an engine of the supersonic combustion ramjet family (scramjet) is developed. Such a design has already been successful in ground tests.

PROPULSION SYSTEMS

Figure 1 illustrates the three basic types of propulsion system for tactical missiles: the rocket, the ramjet, and the turbojet. In the rocket, the propellant is burned in a combustion chamber to produce products of combustion at high pressure (30 to 200 atmospheres) and high temperature (4500 to 7200°F). The burned gases are accelerated to high velocity as they pass through the exhaust nozzle. Thrust is produced by the high pressure acting on the internal surfaces of the motor.

Instead of explicitly defining this pressure field, Newton's law, $F = ma$,* which establishes the equivalency between force and momentum change, is used to determine the thrust from the momentum of the exhaust gases as they leave the nozzle, i.e.,

$$F = \dot{m}u_{ex} + (p_{ex} - p_0)A_{ex}$$

$$= \dot{m}\,[2(h_t - h_{ex})]^{1/2} + (p_{ex} - p_0)A_{ex} \qquad (1)$$

$$\simeq \sqrt{2}\,\dot{m}\,h_t \simeq \sqrt{2}\,\dot{m}\,c_p T_t\,,$$

*See list of symbols on the next page.

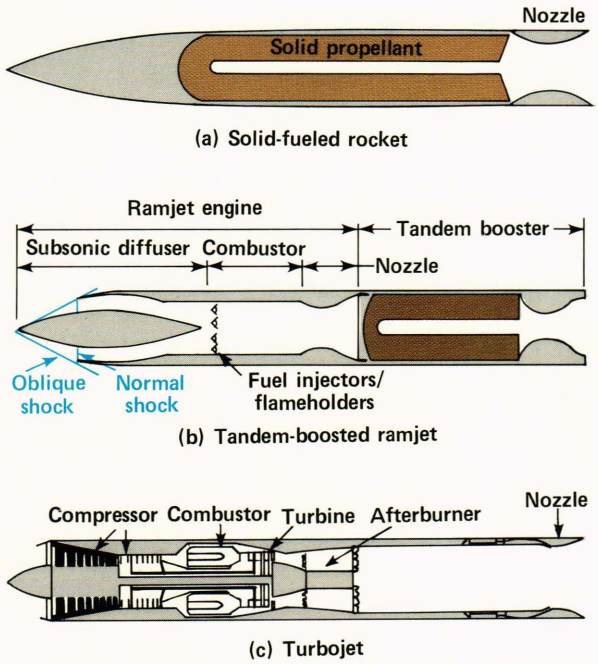

Figure 1 — Propulsion systems for tactical missiles: (a) solid-fueled rocket; (b) tandem-boosted ramjet; (c) turbojet.

SYMBOLS

a	acceleration or constant in burn rate expression, Eq. 4
A_p	surface area of propellant
c_p	specific heat at constant pressure
C_L	lift coefficient
d	diameter
D	drag
ER	equivalence ratio
F	force
g	gravitational constant
h	enthalpy
I_{sp}	specific impulse
L	lift
m	mass
$\dot{m}$	mass flow rate
n	exponent in burn rate expression, Eq. 4
p	pressure
q	dynamic pressure
R	gas constant
t	time
T	temperature
u	velocity
W	weight
x	down-range distance
z	altitude
ϵ	structural coefficient
θ	flight path angle
ν	kinematic viscosity
Π	product function
ρ	density
ψ	elevation angle

Subscripts

b	burnout
c	combustion
ex	nozzle exit
f	final
i	initial or inlet
L	payload
max	maximum value
n	nth stage
p	propellant
R	reference
s	structure
t	total or stagnation
0	free stream or initial

Superscript

*	nozzle throat

where $\dot{m}$ is the propellant flow rate, u is the velocity, p is the pressure, h is the enthalpy, T is the temperature, c_p is the specific heat at constant pressure, subscript t is the stagnation conditions in the rocket motor chamber, subscript ex is the nozzle exit, and subscript 0 is the local ambient. Thus, to produce thrust efficiently, i.e., a large force for a given flow rate or high specific impulse ($I_{sp} = F/\dot{m}$), it is necessary to use propellants that produce gases at high temperatures.

For convenience in handling, rocket-powered tactical missiles generally use solid rather than liquid propellants (Fig. 1a). The propellant is composed of a fuel, an oxidizer (which may be a single chemical compound or a mixture of several ingredients and often contains ignition and burning rate modifiers, catalysts, and inhibitors), and additives to enhance the mechanical and rheological properties (binders, plasticizers, etc.). Typical fuels are organic resins and plastics with or without metal powder additives, typical oxidizers are nitrates or perchlorates, and typical homogeneous monopropellants are the organic nitrates containing fuel and oxidizer in the same substance. Table 1 gives the properties of several typical rocket propellants.

The ramjet (Fig. 1b) differs from the rocket in that air is brought from the atmosphere into the engine to serve as the oxidizer for burning the fuel. The ramjet should be more efficient than the rocket, since it does not have to carry the weight of the oxidizer. On the other hand, this thermodynamic cycle requires compression of the air by slowing it down in the engine inlet prior to heat addition. Such compression is insufficient to produce thrust unless the air speed is greater than about Mach 0.9 (i.e., the speed is 0.9 times the speed of sound). Thus the ramjet must be brought up to this speed or beyond by a booster engine, generally a rocket. The booster can either be a separate stage that is jettisoned after propellant exhaustion, as shown in Fig. 1b, or be integrated with the ramjet, i.e., an integral rocket ramjet. In the latter case, the rocket propellant fills the ramjet combustor during the boost phase, ejectable covers close off the inlet to the combustor, and a rocket throat is used inside the larger ramjet nozzle. After the rocket propellant has been spent and the missile has reached its minimum operating speed, inlet port covers are ejected to permit external air to be captured by the engine inlets and the rocket nozzle insert is ejected.

For speeds between Mach 1 and about Mach 5, the air is compressed by means of a series of shock waves that terminate in a normal shock. The flow into the combustor is subsonic and the engine cycle is called a "conventional" subsonic combustion ramjet. At speeds greater than about Mach 5, a more efficient cycle results if the inlet air is only partially com-

Table 1 — Properties of typical solid rocket propellants.

Propellant	*Metal Content Weight (%)*	*Density (pounds per cubic inch)*	*Flame Temperature (°F)*	I_{sp} *(pounds force-seconds per pound mass)*	*Burning Rate (inches per second)*	*Pressure Exponent n (Eq. 4)*
DB	0	0.058	4100	220 to 230	0.45	0.30
DB/AP/Al	20 to 21	0.065	6500	260 to 265	0.78	0.40
DB/AP-HMX/Al	20	0.065	6700	265 to 270	0.55	0.49
XLDB/AP-HMX/Al	19	0.067	6060	269	0.35	0.50
PVC/AP	0	0.061	4600	230 to 240	0.45	0.38
PVC/AP/Al	21	0.064	5600	260 to 265	0.45	0.35
PS/AP	0	0.062	4700	230 to 240	0.35	0.43
PS/AP/Al	3	0.062	5000	240 to 250	0.31	0.33
PU/AP/Al	16 to 20	0.064	5400 to 6000	260 to 265	0.27	0.15
NEPE	19	0.067	6060	269	0.60	0.50
PBAN/AP/Al	16	0.064	5800	260 to 263	0.55	0.33
CTPB/AP/Al	15 to 17	0.064	5600 to 5800	260 to 265	0.45	0.40
HTPB/AP/Al	4 to 17	0.067	5600 to 5800	260 to 265	0.40	0.40
PBAA/AP/Al	14	0.064	5400 to 6000	260 to 265	0.32	0.35

Al	Aluminum
AP	Ammonium perchlorate
CTPB	Carboxy-terminated polybutadiene
DB	Double base
HMX	Cyclotetramethylene tetranitramine
HTPB	Hydroxy-terminated polybutadiene
NEPE	Nitrate ester plasticizer
PBAA	Polybutadiene-acrylic acid polymer
PBAN	Polybutadiene-acrylic acid-acrylonitrile terpolymer
PS	Polysulfide
PU	Polyurethane
PVC	Polyvinyl chloride
XLDB	Cross-linked double base

pressed and enters the combustor with a speed greater than Mach 1. This cycle is called a supersonic combustion ramjet.

The third basic engine cycle is the turbojet (Fig. 1c). A rotating air compressor is added ahead of the combustor to circumvent the low speed limitation of the ramjet, and a turbine to drive this compressor is added behind the combustor. The turbomachinery more than pays for itself in weight at subsonic and low supersonic speeds because the Carnot efficiency of the engine is much greater than the compressor "expense" as long as sufficient heat can be added in the combustor. However, at speeds above about Mach 3, the adiabatic compression of the air in the inlet raises its temperature to a point where only a relatively small amount of heat can be added in the combustor without damage to the turbine blades from overheating. Moreover, the relatively heavy compressor is no longer needed, and the cycle becomes less efficient than the ramjet.

RAMJET DESIGN TYPES

Many variations and combinations of these basic cycles have been used; typical examples are shown in Fig. 2. Figure 2a is a solid-fueled air-ducted rocket with an integral rocket booster. In the configuration shown, multiple axisymmetric aft-entry air inlets are used. Variations include half-round and two-dimensional inlets, perhaps with inward-turning compression surfaces. Depending on the thrust required and the constraints that may be imposed by the stowage of the missile, one, two, or four air inlets can be used. After the booster propellant has been expended and the small rocket nozzle and air inlet covers have been ejected, the sustain propellant is ignited to produce a hot fuel-rich exhaust that is burned to completion with the captured air in the main combustor. As contrasted to the ramjet where a sheet metal can or metal baffle obstructions are used to stabilize the flame, flame stabilization in this design occurs in recirculation zones that are generated in the region of the air intake ports. Since the solid propellant contains some oxidizer, the specific impulse, $I_{sp} = F/\dot{m}$, is lower than for the pure ramjet. However, the relatively high density of the solid fuel provides a high packaging efficiency that is an important consideration in volume-limited situations.

Figure 2b is an integral rocket liquid-fueled supersonic combustion ramjet. A "chin" inlet is shown that takes advantage of a favorable forebody compression field at angle of attack in the plane of symmetry. On the other hand, bank-to-turn rather than skid-to-turn control is required, which can have detrimental effects on the guidance system accuracy, especially during terminal maneuvers. Rather than a single ejectable nozzle, multiple nozzles are shown, reducing volume at the expense of weight and complexity.

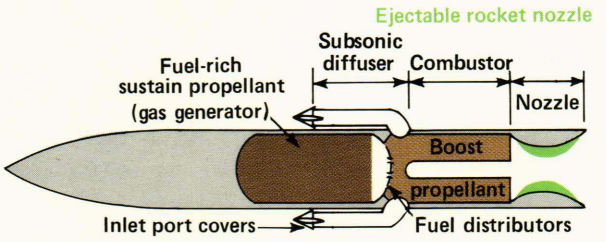

(a) Solid-fueled ducted rocket

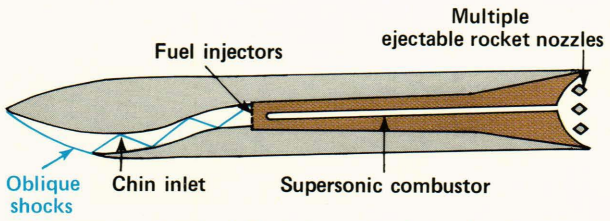

(b) Integral rocket liquid-fueled supersonic combustion ramjet

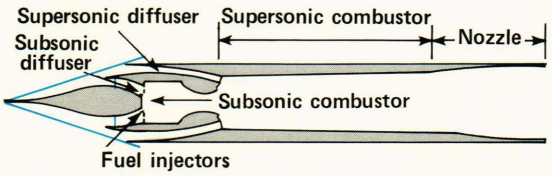

(c) Liquid-fueled dual-combustor ramjet

Figure 2 — Variants of basic propulsion cycles: (a) solid-fueled ducted rocket; (b) integral rocket liquid-fueled supersonic combustion ramjet; (c) liquid-fueled dual-combustor ramjet.

When the rocket propellant is consumed and the nozzles and inlet port covers have been ejected, liquid fuel is injected from the walls into the combustor unencumbered by flame holders that would produce undesired shock losses in the supersonic flow. Since the flow is supersonic, the residence time in the combustor is very short. Therefore, to burn conventional fuels, either the flight Mach number must be high, i.e., above Mach 5, or a highly reactive fuel or fuel blend, such as a hydrocarbon with 20% ethyl decaborane, must be used. Figure 3 is a photograph of a scramjet engine that was developed at APL and tested in the free-jet facilities at the Navy's Ordnance Aerophysics Laboratory in Daingerfield, Tex., at Mach 5 and 6 in the late 1960's and in the APL Propulsion Research Laboratory (PRL) at Mach 7 in 1970-71.

An alternative technique to reactive fuels is to inject simultaneously a highly reactive oxidizer, e.g., chlorine trifluoride (ClF_3), with a conventional fuel at the expense of simplicity, increased safety hazard, and loss in specific impulse.

An engine concept that bridges the gap between the supersonic and hypersonic speed ranges, with logistically acceptable fuels, is the dual-combustor ramjet, shown in Fig. 2c. A portion of the airflow captured by the inlet is diverted to a hot-gas generator, which,

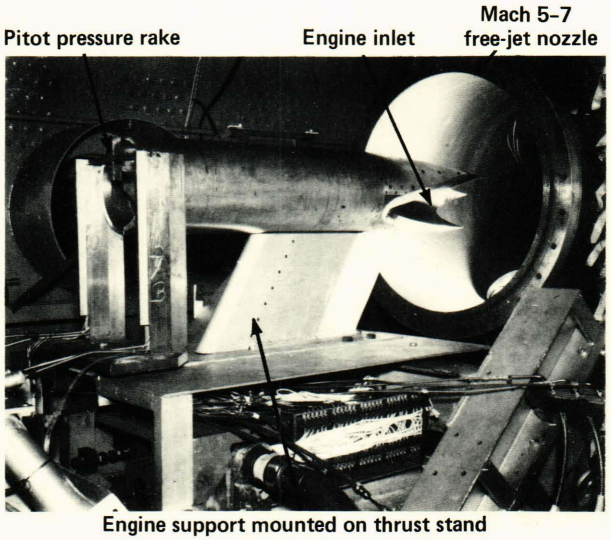

Figure 3 — A Navy/APL heat-sink type scramjet engine model in position for a hypersonic test.

in fact, is a "dump-type" subsonic combustor. To simplify the fuel control and injection system, all of the fuel is injected into the gas generator. Consequently, this combustor must operate considerably in excess of stoichiometry when high thrust is demanded. The hot fuel-rich combustion products pass into the main supersonic afterburner to complete the heat release by reacting with additional air.

Both this engine cycle and the scramjet (Fig. 2b) can, in fact, be dual-mode engines: they can operate in either the subsonic or the supersonic combustion mode. At low flight Mach number and high equivalence ratio, *ER* [*ER* = (fuel/air)/(fuel/air) at stoichiometry], a normal shock is located in the combustor entrance and heat release begins in subsonic flow. Heat addition occurs simultaneously with pressure drop in a diverging duct that accelerates the flow through the sonic point to supersonic conditions at the combustor exit. The price that is paid for the versatility in operation over a wide speed range is the complexity and weight of the split flow inlet compression system and gas generator. Figure 4 includes a schematic illustration and a photograph of the gas generator/supersonic afterburner currently being tested at PRL.

The particular choices of inlet type (e.g., chin, axisymmetric nose, or side mounted), nozzle type (single or multiple), and booster type (tandem or integral) in the configurations shown in Fig. 2 were arbitrary. Indeed, nearly every possible combination of these components has been examined for one or more applications. Moreover, Fig. 1a depicts only the simple, single-stage rocket. As the subsequent discussion will show, in some applications the optimum rocket missile may either have two stages or a propellant designed to burn intermittently in two or more pulses.

SELECTION OF PROPULSION CYCLE

Selection of the optimum propulsion cycle for a given application can be an arduous task. Generally,

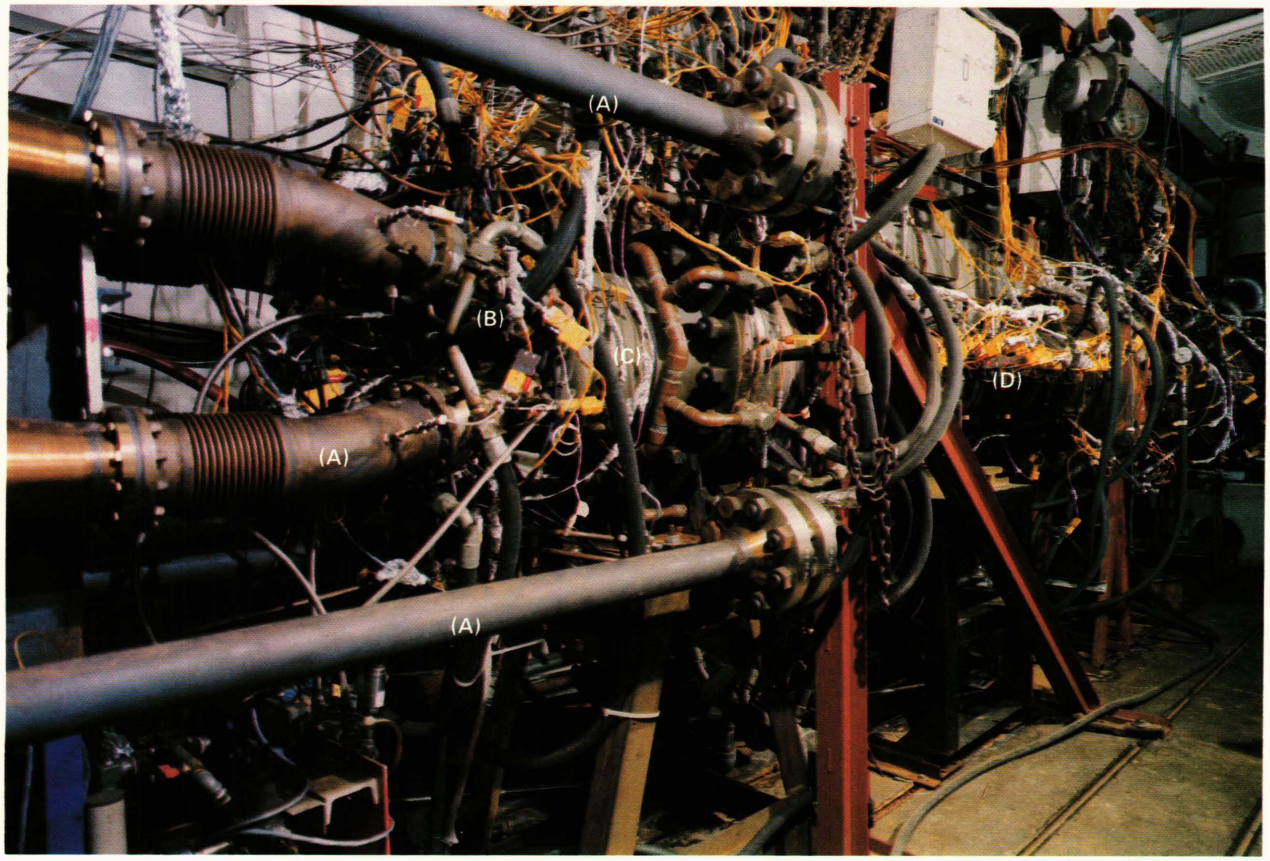

Figure 4 — Dual-combustion ramjet direct-connect test apparatus.

many cycles can be eliminated by a cursory examination, but the final selection often requires a detailed composite design. Even then, the selection may be ambiguous; one cycle may be better for a particular mission, but another may have the versatility to carry out several missions. There may be a trade-off between cost and performance, etc.

Two relatively simple expressions can provide some insight into the factors that ultimately lead to the selection of the candidate engine cycles. The first is the Breguet range equation, which holds for the simple case of cruising at constant velocity u with the lift L equal to the weight W, viz.,

$$R = uI_{sp}\ (L/D)\ \ln\frac{W_i}{W_f}\,, \qquad (2)$$

where D is the drag and W_i and W_f are the weights at the beginning and end, respectively, of the cruise phase.

The second expression is for the velocity change of a vehicle during the climb and acceleration phase, viz.,

$$u_b - u_0 = g\,I_{sp}\ln\frac{W_0}{W_b} - \int_0^b \left(g\sin\theta + \frac{D}{W}\right)dt\,, \qquad (3)$$

where W_0 is the initial weight ($W_S + W_P + W_L$), W_S is the structural weight, W_P is the weight of the propellant, W_L is the payload weight, $W_B = W_S + W_L$ is the burnout weight, g is the acceleration due to gravi-

ty, and θ is the local flight path angle with respect to the horizontal.

In both expressions, performance (either the range or the accelerative ability) is directly related to the specific impulse, I_{sp}. Typical values of I_{sp} for the propulsive cycles depicted in Figs. 1 and 2 are shown in Fig. 5. The values are based on the use of conventional hydrocarbon fuels in the airbreathing engines. The turbojet is the most efficient for speeds up to Mach 2.5, which has led to its near universal use as an aircraft powerplant. If relatively high thrust is required, the turbojet operates with an afterburner and I_{sp} is significantly lower.

Most missile applications require high thrust. As a result, the high cost of the turbomachinery for an expendable engine eliminates the turbojet from consideration unless long range is the dominant requirement and high acceleration and high speed are not mandatory. The current generation of cruise missiles (Harpoon and Tomahawk) are in this category. In the supersonic to moderate hypersonic speed range, the ramjet is attractive despite the booster requirement to bring it up to speed. The choice among subsonic-combustion, supersonic-combustion, or dual-combustor ramjets depends on the velocity requirement for the mission as well as cost and logistic considerations, as noted earlier.

As shown in Fig. 5, the rocket's specific impulse is only 20 to 30% of that of a ramjet. On the other hand, the mass fraction of propellant for a rocket for a tactical missile is typically 50 to 70% of the initial weight as compared to 25 or 35% for the ramjet. Thus the logarithmic terms in Eqs. 2 and 3 are larger by a factor of 2.5 to 2.8 for the rocket. Since the product of the two terms is significantly lower for the rocket, this generally eliminates it from consideration if long range during cruise is required (Eq. 2). However, during rapid acceleration the second term in Eq. 3 can be significant. This term is minimized when dt is small and drag is not too large, which corresponds to a relatively high average thrust to weight ratio, (F/W), of about 10. By tailoring the grain design and using a relatively large exit nozzle throat, it is possible to design a rocket with F/W of about 10, which is essentially independent of altitude. High-speed ramjets can be designed with F/W of about 10 near sea level. But since the thrust is proportional to the ambient pressure, at an altitude of 50,000 feet F/W is approximately 1 and at 100,000 feet about 0.1. Thus, if the missile must climb to high altitude while accelerating rapidly and a long cruise range is not required, the rocket may be the preferred engine.

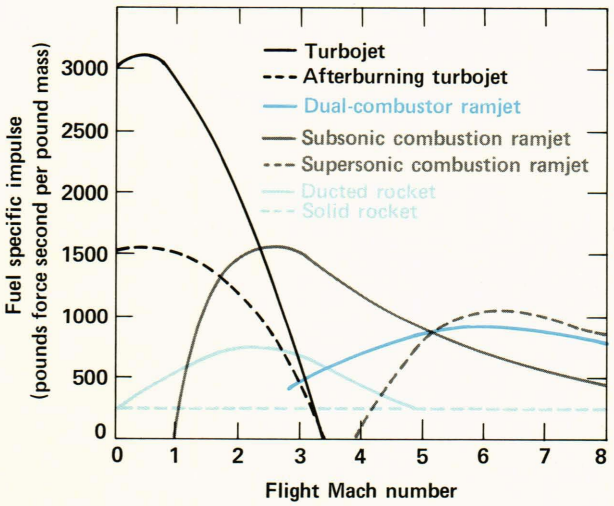

Figure 5 — Fuel specific impulse for various missile propulsion systems.

To develop this argument further and to give some insight into the design of propulsion systems, it is necessary to examine families of climb-out and cruise trajectories. For a given mission objective and constraints inherent to the composite design of the missile, e.g., structural and control limitations, the climb-out trajectory can be optimized by the introduction of lateral aerodynamic force and modulation of the thrust. Lateral force, which affects the missile attitude θ, can only be generated at the expense of induced drag, so the terms within the integrand of Eq. 3 are coupled. Moreover, drag increases with the square of velocity and decreases exponentially with altitude Z. Thus, rapid acceleration reduces dt but not necessarily $\int (D/W)\,dt$. No general solution has been found for Eq. 3, nor is there a rigorous procedure for optimization of the climb-out. However, considerable attention has been directed toward suboptimal schemes[1,2] that use high-speed computations to obtain apparent optimal trajectories for particular missile configurations and missions.

The interdependence of the missile composite design and the optimization of the trajectory will become apparent as particular mission requirements are examined. Typical trajectories for the first generic class of missions to be examined are depicted in Fig. 6. In this case, the missile is to be launched vertically ($\theta \approx 90°$) from a canister, after which it will climb, accelerate, and intercept a target at an altitude Z_A. The criterion for selecting the best propulsion system is maximum velocity at point A, which in general corresponds to minimum flight time.

Consider first the case of a solid propellant rocket. Let us hypothesize that it will be possible to select propellant grains and specify grain shapes and nozzle sizes that will produce constant flow rates of the propellants. Trajectories can now be flown for different flow rates to determine whether flight time is dependent on them. Curve I in Fig. 6 corresponds to a high flow rate, a short duration turn from the vertical, and a zero-lift ascent trajectory, i.e., no normal aerodynamic force is applied. Thus, the vehicle flies ballistically. Maximum velocity is reached when the propellant burns out and the missile coasts with some slowdown from burnout to altitude Z_A.

Curve II is for a lower flow rate. Burnout occurs later at a higher altitude and the trajectory "falls over" farther from the vertical because the velocity during the early phase of the climb-out is lower than

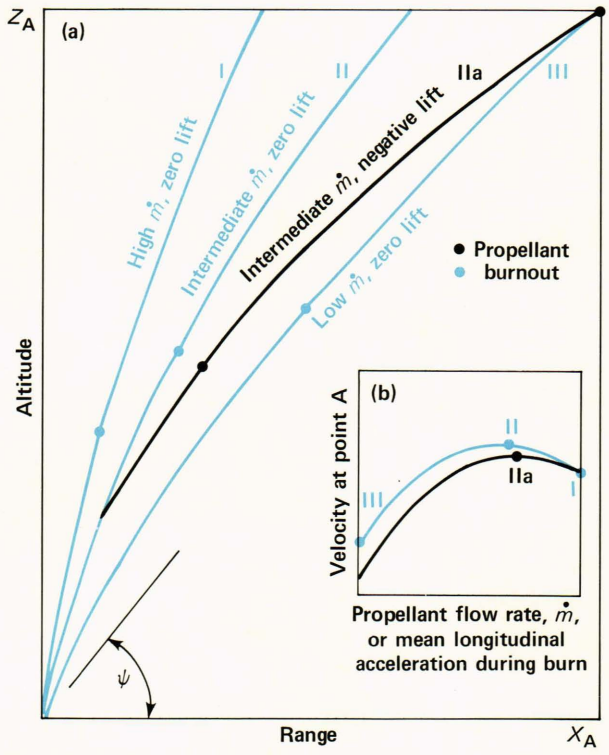

Figure 6 — (a) Ascent trajectories of missiles for target intercept near point A, and (b) determination of optimum propellant flow rate.

for curve I. Curve III is for the lowest flow rate covered in this example. Burnout occurs nearer X_A, Z_A and the trajectory falls over somewhat farther.

By introducing negative aerodynamic lift, it is possible to force trajectories I and II to pass through X_A, Z_A also, as typified by curve IIa for the intermediate value of flow rate. Similarly, trajectories II and III could be forced to pass through the terminal point of trajectory I by introducing positive lift.

Regardless of whether a comparison is made for ballistic ascent trajectories or for lifting trajectories forced to pass through the same point in space, there exists a propellant flow rate that yields a maximum mean velocity, as shown in Fig. 6b. The optimum trajectory corresponds to the case where the integrand in Eq. 3 is minimized. This can best be understood by examining the limiting case of $\dot{m} \rightarrow \infty$, which, from Eq. 3, would produce the maximum velocity immediately after launch. However, the vehicle would experience rapid slowdown due to the high drag at low altitude. With a lower flow rate the missile would climb through the dense lower atmosphere at a lower velocity with lower drag impulse, taking the same time to arrive at an intermediate altitude but with higher velocity.

As an example, consider the case of a rocket weighing 4000 pounds at lift-off, of which two-thirds is propellant that produces an average I_{sp} of 260 pound force seconds per pound mass. The rocket is 18 inches in diameter and 230 inches long, and has a low-drag nose. Taking the unrealistic limiting case of instantaneous burning of the propellant, the burnout velocity would be 9190 feet per second. For a vertical climb, the rocket would reach an altitude of 95,300 feet in 11.99 seconds with a velocity of 7500 feet per second, and an altitude of 204,100 feet at a velocity of 7000 feet per second. For ascent trajectories to targets having elevation angles less than the zenith, the corresponding altitudes at these velocities would be lower because the drag impulse would be higher.

As shown in Fig. 7, there is a range of finite values of propellant flow rates that yields a higher Z_A for a corresponding velocity on a vertical climb. For clarity, the entire $\dot{m} = \infty$ curve is not included. Curves drawn through the loci of points on ascent trajectories corresponding to velocities of 7500 and 7000 feet per second are shown for flow rates from 60 to 200 pounds per second. It is clear that only when targets are near the zenith are high flow rate values desirable. For targets below an elevation angle of about 30°, the optimal flow rate is about 80 pounds per second.

Unless the enemy uses ballistic missiles against ships, the primary role for defense of the Fleet from air attack is from targets at angles below 30°. Consequently, the emphasis will be on propulsion systems designed to cope with this threat. For the case with a constant flow rate of 80 pounds per second, the propellant burn time is 33.3 seconds and the burnout velocities vary from 7260 feet per second for targets at low elevation angles to 7858 feet per second for targets at elevation angles of about 35°. For an evaluation angle of 90°, the burnout velocity drops to 7770 feet per second, which again shows the interaction of the terms within the integrand in Eq. 3. This range of burnout velocities corresponds to a mean longitudinal acceleration during burning, u_b/gt_b, of 6.76 to 7.32 g where t_b is the time at burnout. Although each missile design and mission would have a unique flow rate value, the value that yields a mean acceleration of 5 to 10 g is typical of a wide variety of cases.

Granting that a constant flow rate of 80 pounds per second is a reasonable design point from which departures can be made to examine other effects, the case of nonconstant flow rate can be studied. Two cases are considered: a constant flow rate with an intermediate period without burning and a linear variation of flow rate with time. Figure 8 shows the effect of interrupting the burning of the propellant for periods of 5 to 40 seconds once the vehicle reaches a velocity of 5000 feet per second. For the range of elevation angles of primary interest, pulses up to 30 seconds lead to increases in performance, i.e., the u_A = 7000 feet per second contour is moved farther from the launch point. The shift of the curve for altitudes below 120,000 feet for the 30 seconds pause corresponds to a slowdown of about 400 feet per second for the steadily burning case. Lengthening the pulse beyond 30 seconds causes too great a slowdown to move the contour further and, indeed, if the pulse is long enough the vehicle cannot reach 7000 feet per

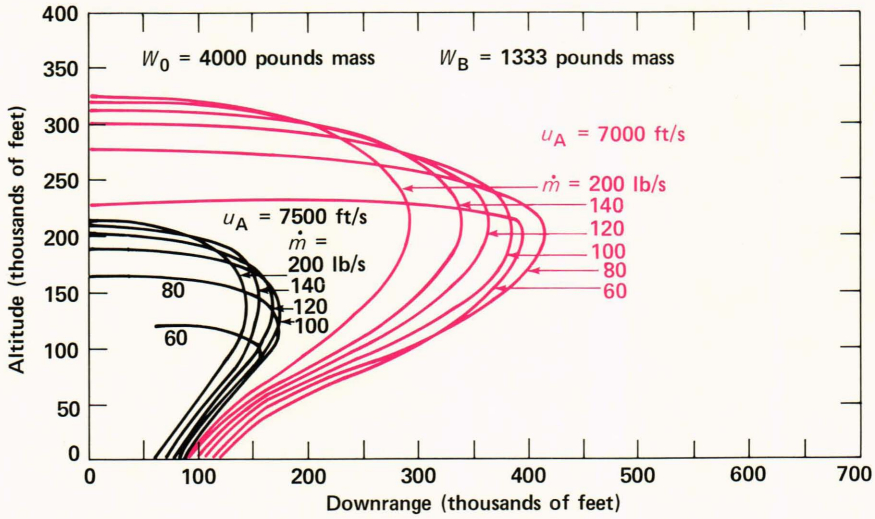

Figure 7 — The effect of propellant flow rate on ascent trajectories.

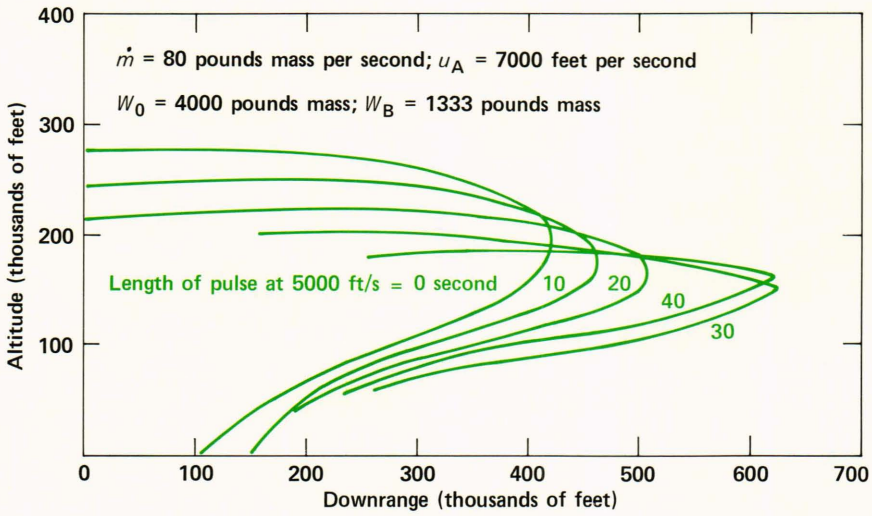

Figure 8 — The performance of pulsed rocket motors.

second. The choice of 5000 feet per second for the point at which the zero flow rate pulse is initiated is about optimum for extending the u_A = 7000 feet per second contour for pulse lengths of 30 seconds. Had the pulse been delayed until u_A = 6000 feet per second, only about half of the gain would have been realized. Whether the added complexity of the motor design to accommodate pulsing is warranted would depend on how crucial the additional performance is in meeting mission requirements. The amount of payload that would have to be replaced by additional propellant to produce an equivalent extension of the 7000 feet per second contour, would be about 85 pounds.

A plot similar to Fig. 8 can be used to compare the performance of linearly varying flow rates with constant flow rates. The 80 pounds per second constant flow rate case is again used as reference. Four cases were examined: linearly increasing flow rates from 60 to 100 pounds per second and from 70 to 90 pounds per second and linearly decreasing flow rates over the same two ranges. As shown in Fig. 9, increasing flow rates degrade performance, whereas decreasing flow rates extend the 7000 feet per second contour.

Unfortunately, from the point of view of grain design, a so-called "regressive" burning rate is difficult to achieve. Figure 10 shows typical cross sections of some radially burning propellant grains. The simplest configurations, shown in Fig. 10a, result in increasing flow rates as the diameter and area of the burning surface(s) increase with time. To obtain a near constant or decreasing flow rate, more complicated internal shapes are required, as shown in Fig. 10b, introducing problems of high stress concentrations in corners and the possibility of producing longitudinal slivers of propellant that could be sheared off and expelled from the rocket chamber without burning.

An "end burning" grain could also produce a constant flow rate, but the required burn rates for the propellant would have to be increased significantly. For a flow rate of 80 pounds per second, the volumetric burning rate for a propellant having a density of 0.067 pound per cubic inch would be 1194 cubic inches per pound. For a grain having a diameter of

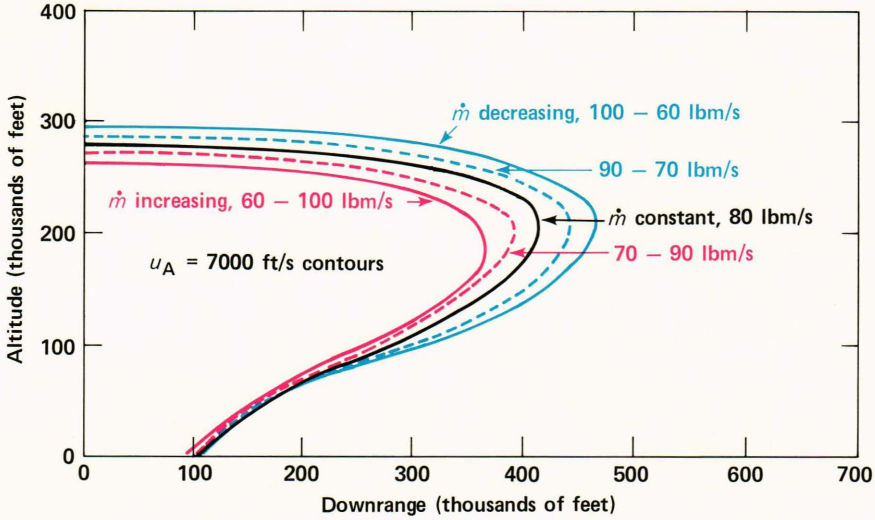

Figure 9 — The effect on rocket motor performance of linearly varying the weight flow of propellant.

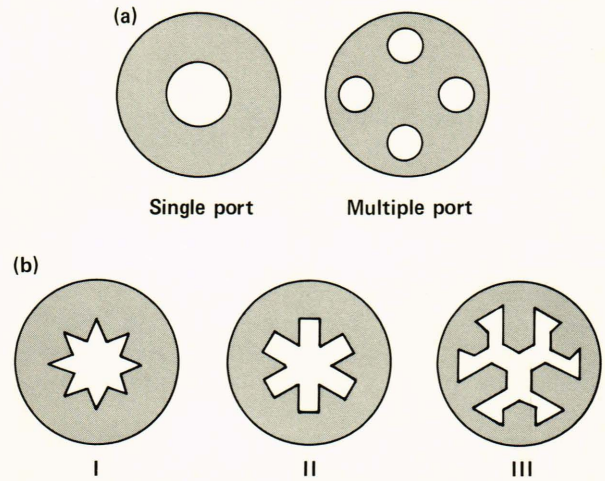

Figure 10 — Cross sections of typical solid propellant grains: (a) progressive burning rate designs; (b) near-neutral (I) and regressive (II and III) burning rate designs.

about 17.5 inches, this would require a linear burning rate of about 5 inches per second, about an order of magnitude larger than can be obtained with the propellants shown in Table 1. The addition of longitudinal metallic wires in the propellant offers the possibility of increasing the burning rate, perhaps to the level required.

The internal star designs have surface areas ranging from 1 to 5 Dl , where D and l are the overall diameter and length of the grains. Assuming that grain length is two-thirds of the 230-inch missile length, the corresponding range in required burning rates would be 0.09 to 0.45 inch per second, which is in the range that can be obtained with the Table 1 propellants.

The burning rate of most propellants is in accordance with Saint Robert's law, viz.,

$$\dot{m} = a A_p \rho_p P_c^{\,n} , \qquad (4)$$

where the lead coefficient a is constant for a given grain temperature. Combining this expression with the equation for flow through a sonic throat, viz.,

$$\dot{m} = p_c A^* u^* / R T^* , \qquad (5)$$

shows that for a fixed nozzle, i.e., A^* constant, and propellant temperature (T^*, u^* constant),

$$A_p \approx (\dot{m})^{1-n} . \qquad (6)$$

The asterisks refer to conditions at the throat of the nozzle. To obtain a regressive burning rate of from 100 to 60 pounds mass per second, the range of percentage reductions in A_p would be from 29 to 54% for the propellants listed in Table 1. The internal star design shown on the right in Fig. 9 would have an A_p that decreases by about 60%. Either this or a somewhat less complex shape could presumably meet the regressive rate selected in the example.

There is a mitigating effect that was not considered in this example, viz., that the structural weight of the linearly varying propellant flow engine would be greater than that of the constant propellant flow engine because the design maximum pressure would be greater. Consequently, most missile designs tend to use burning grain designs that generate gases at approximately a uniform rate.

The trend of these results suggests that for two-stage rocket designs, the flow rate of the first stage should be greater than that of the second stage. To establish this point, it is necessary to examine the differences in performance for two-stage vehicles where flow rate is varied for the two stages. A complete examination of this issue is an arduous task; however, some exemplary results can be discussed that show the general trends that would result from a more thorough investigation. Classical theory (see, e.g.,

Ref. 3) shows that for vehicles having multiple stages, Eq. 3 must be revised to determine the velocity change for an accelerating vehicle. In this case the logarithmic term becomes

$$\ln \left[\prod_{1}^{n} (W_{0i} / W_{bi}) \right] , \qquad (7)$$

where the bracketed term is the product of the n weight ratios of the i individual stages. In general, the burnout velocity of the nth stage u_{bn} is greater than the burnout velocity for a single-stage vehicle having the same ratio of payload to initial weights, W_L / W_0. The higher velocity is a result of discarding the structural weight of the burntout stage at staging, thereby saving the propellant that would have been used to accelerate this mass. For the large velocities required for long-range ballistic missiles and space vehicles, staging is mandatory for high W_L / W_0. Three- and four-stage vehicles are typical for these missions. For tactical missiles the velocity increment is typically one-third to one-half of that required for ballistic missiles, and no more than two stages are required.

Analytical solutions (see, e.g., Ref. 3) to maximize the burnout velocity for particular propulsive and structural characteristics have been found that show, for the idealized case of drag-free/gravity-free climbout of a vehicle having equal I_{sp} and structural coefficients $\epsilon = W_{si} / (W_{si} + W_{pi})$ for all stages, each stage should have the same weight fraction and therefore produce the same velocity increment as every other stage. Here, W_{pi} is the weight of propellant in the ith stage. When drag, gravity, varying I_{spi}, and ϵ_i are considered, the optimum u_{bi} for rocket-powered vehicles occurs when the velocity increment of the stage increases with each succeeding stage. Figure 11 shows that optimum performance for two-stage rockets is obtained when the velocity increment of the first stage is 44 to 46% of the total Δu.

The same trend would also be observed when the second stage is an airbreathing missile. However, this cannot be fully exploited with the fixed geometry engines that are generally used in tactical missiles. Usually it is not possible to design a fixed geometry engine (i.e., the inlet area and the throat of the exhaust nozzle cannot be varied) that will operate over a velocity range below 55 to 60% of the maximum velocity, as shown in Fig. 11b. If variable geometry is practical, the velocity increment of the first stage can be reduced to about 46 to 48% for optimal performance.

A 4000-pound missile with similar characteristics as before, except that it has two stages rather than one, can now be reexamined. If a structural coefficient $\epsilon_i = 0.1$ is taken for the rocket motor case, not including the nozzle and thrust vector control system, 1480 pounds of propellant should be packaged in the first stage to obtain $u_{b_1} \approx 0.45\, u_{b_2}$. At first-stage burnout the total weight would be 2520 pounds, of which 214 pounds would be dropped (164 pounds of rocket motor case and about 50 pounds of nozzle, thrust vector control, and stage clamping devices). The second stage would have an initial weight of 2306 pounds, including 1153 pounds of fuel, 122 pounds of structure, and 20 pounds of nozzle. Thus, both missiles would have effective payload weights of 1006 pounds if it is assumed that the nozzle thrust vector control of the one-stage vehicle is 30 pounds. The effective payload includes the warhead and guidance radome, the forebody, and all other components of the engine other than the rocket motor.

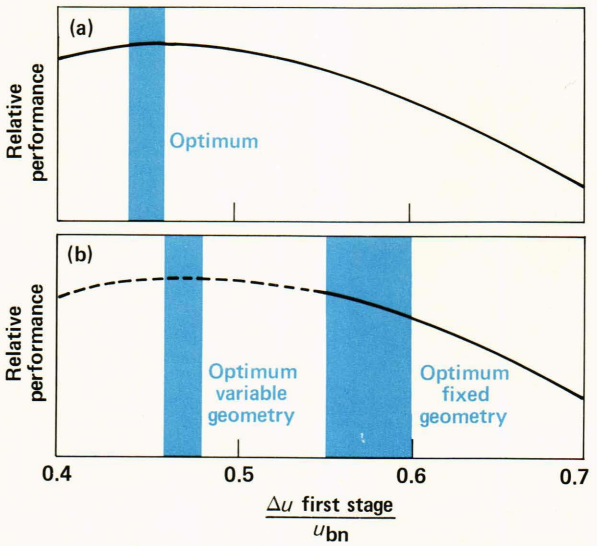

Figure 11 — Optimal staging of tactical missiles: (a) two-stage rocket; (b) rocket booster, airbreathing second stage.

Comparing the performance of one- and two-stage rockets for altitude values of 120,000 feet or lower shows that the u_A = 7000 feet per second curve for the two-stage rocket would extend about 20,000 feet farther when the flow rates are 80 pounds per second for both stages. This increment would about double if the mass flow rates were optimized, i.e., 140 and 60 pounds per second for the respective stages. Again, whether the added cost and complexity would be warranted for a Fleet defense missile targeted at low elevation angle is questionable. On the other hand, for targets at high elevation angles, a two-stage vehicle would be capable of reaching nearly double the range at the same burnout velocity for a given elevation angle.

The domain of velocity values examined so far, i.e., equal or greater than 7000 feet per second, precludes meaningful direct comparisons of rockets and airbreathers since, at present, structural and perhaps propulsive constraints appear to be too formidable to reach these speeds in tactical airbreathing missiles. However, the 4000 to 6000 feet-per-second velocity interval is of considerable interest for Fleet air defense.

Two approaches are possible to compare the performance of rockets and airbreathers in this range. The first is to compare an airbreather capable of

reaching u_A = 6000 feet per second with the rocket over a range of velocity values up to 6000 feet per second. The second is to compare a family of airbreathers, each designed for a particular maximum value. For velocity values less than 6000 feet per second, the latter approach would show better performance for the airbreathers because more of the total weight of the system could be put in the second stage. For example, to meet the u_{b_1} criterion shown in Fig. 11 for a fixed geometry airbreather capable of reaching u_A = 6000 feet per second would require a booster weighing about 1960 pounds, whereas for a u_A = 4000 feet per second missile the booster weight would be about 1259 pounds. Again, these designs are for total weights of 4000 pounds and many assumptions have been made regarding structural weights and other factors.

The procedures used to optimize the airbreather stages and trajectories are complex and the reader is referred to more detailed discussions of the subject (see, e.g., Ref. 4). Suffice it to say that the geometry of the engine, the modulation of thrust during climb-out, and the variation of normal force all enter into the optimization.

The final result of the comparison is shown in Fig. 12 where the single-stage rocket is compared with a family of optimally designed airbreathers for the mission described in Fig. 6, which, from a guidance system point of view, would correspond to commanding the missile by way of a shipboard radar. In Fig. 12, the down-range scale has been compressed. The rocket is the preferred engine for all elevation angles above 10°. The region for the rocket is terminated since, at high altitude, control of the missile would have to be provided by a means other than aerodynamic surfaces. The 160,000-foot limit shown here corresponds to a dynamic pressure q of 45 pounds per square foot for a velocity of 6000 feet per second. Control at lower dynamic pressure would have to be provided by auxiliary thrusters; this not only greatly complicates the missile design, but thrusters generally are not available in tactical missiles. The airbreather is preferred for all velocities that can be reached at $Z_A < Z_{A_{max}}$ prior to fuel exhaustion, since the airbreather still has fuel remaining to maintain a high velocity, whereas the rocket is coasting. The airbreather operating envelope is terminated at fuel exhaustion and at $Z_A = Z_{A_{max}}$, which corresponds to the altitude above which stable combustion cannot be obtained.

Trajectories representative of a second generic class of missions are shown in Fig. 13. Here the objective is to obtain maximum range by accelerating and climbing to an altitude Z_c and cruising in near horizontal flight from c to d. As in the previous example, the rocket has a maximum speed greater than the airbreather. The propellant is consumed relatively early in the climb-out, i.e., 33.3 seconds into a climb-out of about 100 seconds, and the vehicle decelerates following burn-out. To obtain maximum range, the flight path during climb-out and approach to the cruise condition must be optimally shaped. In general, the optimal path corresponds to launch near the vertical (θ = 90°) and continual turn-down (negative lift) up to the apogee. If near vertical launch is not achievable, positive lift (and thrust vector control) are used during the early phase of the climb-out to bring the vehicle close to the $\theta = f(z)$ characteristic of the optimal vertical launch case.

The types of trajectories that must be examined to obtain optimal range of a high thrust-to-weight (F/W) ratio vehicle (e.g., the rocket) are typified by curves IV, IVa, and V in Fig. 13. A high F/W vehicle has the accelerative capability to "overshoot" Z_c and then glide from the apogee back to Z_c by a number of possible paths with the introduction of positive lift. Curve IV corresponds to a case with a lift-to-weight ratio (L/W) > 1 as Z_c is approached. With L/W = 1

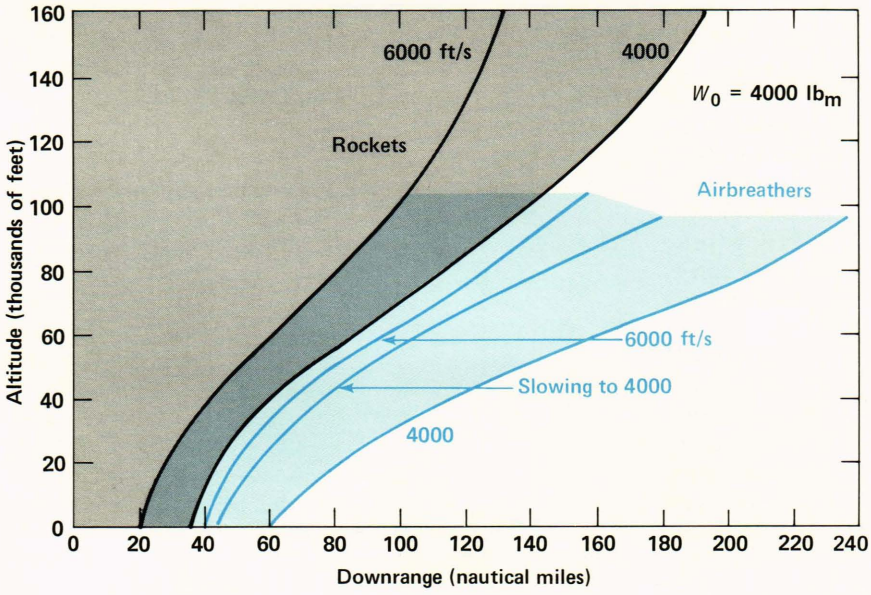

Figure 12 — Comparison of rockets and ramjets for area defense mission.

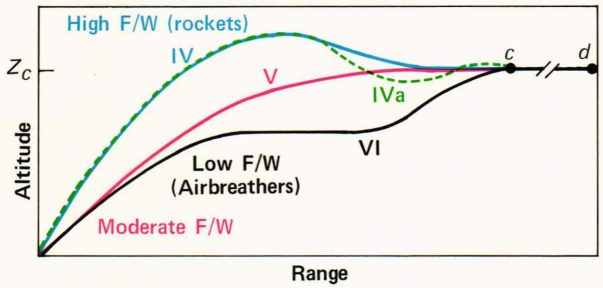

Figure 13 — Effect of thrust-to-weight ratio on ascent trajectories for missiles designed for near-level flight at an altitude Z_c.

at Z_c the vehicle will oscillate about Z_c with a decreasing excursion as time progresses, as typified by curve IVa. With $L/W < 1$, the vehicle can approach Z_c at $\theta = 0$ asympotically from below (not shown). The permissible altitude at apogee is limited to the aforementioned requirement to maintain control but, in general, optimal range is obtained on trajectories having lower apogees. These constraints significantly restrict the region of permissible climb-out trajectories to a narrow corridor in ψ_a, where ψ_a is the elevation angle of the apogee with respect to the launch point. For example, given that the flow rate is 80 pounds per second and that the rocket is constrained to an apogee of 100,000 to 160,000 feet, then the range in elevation angle is from 11 to 15°.

Curve V of Fig. 13 schematically represents the climb-out of a rocket with a moderate thrust-to-weight ratio or of a ramjet having a relatively large ratio of inlet areas to body cross-sectional area. For the same Z_c, however, the optimal climb-out for an airbreather would lie below that of a rocket. That is a consequence of the need to optimize thrust and fuel flow-rate simultaneously with the minimization of the integrand in Eq. 3 in the climb-out of an airbreather. Typically, those trajectories require modulation of the lateral force that produces turn-down following launch, followed by positive lift at low and intermediate altitudes, and negative lift as Z_c is approached.

Curve VI is representative of the climb-out of a low thrust-to-weight ratio engine. The accelerative capability is inadequate to climb to Z_c and accelerate to the desired u_c simultaneously. Instead, the vehicle must climb to a lower altitude, use lift to maintain this altitude, accelerate to u_c, then turn up with $L > W$, and finally approach Z_c with $L < W$. Usually this type of climb-out results in poorer performance than a Case V climb-out, which is one of the factors that influences the choice of the proper thrust-to-weight ratio propulsion system.

Optimal cruise range for the airbreathers or glide range for the rockets usually results when the vehicle flies from c to d at an angle of attack corresponding to $(L/D)_{max}$. The maximum lift-to-drag ratio varies with the aerodynamic configuration, velocity, and altitude, but for tactical missiles in the range of 4000 to 7000 feet per second, $(L/D)_{max} \approx 3$ and the corresponding angle of attack α is between 8 and 12°. During cruise the rocket is lighter than the airbreather, and the optimum altitude at the same velocity is somewhat higher. As the rocket slows down during the glide, the optimum altitude decreases. On the other hand, as the airbreather burns fuel to maintain constant velocity, the optimum altitude increases with the decreasing weight unless that altitude is too high to permit efficient operation of the inlet and combustor.

Figure 14 shows the altitude-range envelope for points d for the same tactical missiles used for the flight envelope of Fig. 12. For the rocket, boundaries are shown for slowdown to u_d = 4000 and 6000 feet per second. For the airbreathers, three boundaries

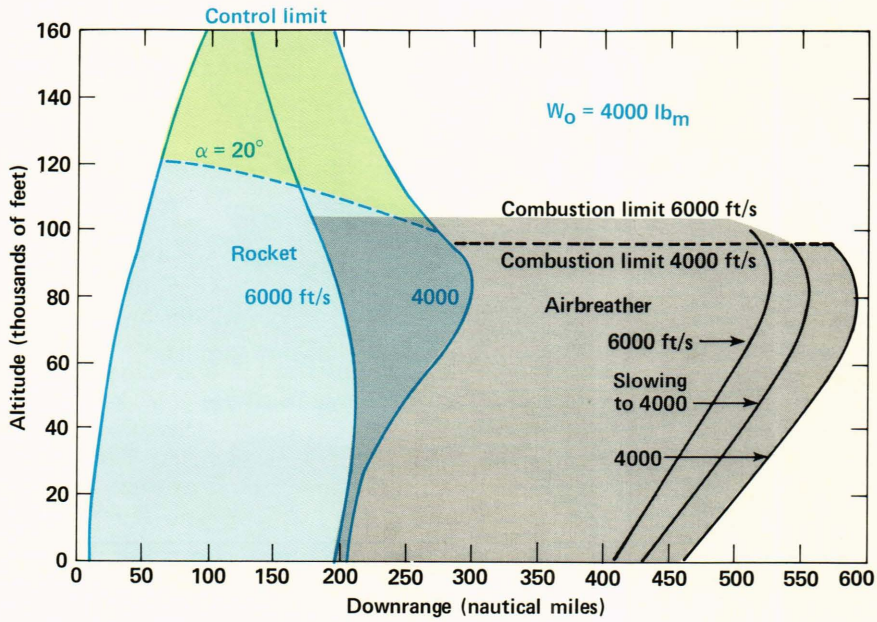

Figure 14 — Comparison of rockets and ramjets for long-range cruise missions.

are shown. The area above the dashed line is shaded in green to show that angles of attack greater than 20° would be required to maintain level flight of a coasting rocket. Indeed, at altitudes above about 130,000 feet, level flight is not possible for this vehicle. The u_d = 6000 feet per second is for a missile designed to cruise at 6000 feet per second. Two 4000 feet-per-second boundaries are shown; the one having the greatest extent is for a missile designed to cruise at 4000 feet per second and the other is for the 6000 feet-per-second design, coasting to 4000 feet per second following fuel exhaustion.

As in Fig. 12, the range that can be reached by the airbreathing missile is considerably greater than that reached by the rocket. On the other hand, for ranges less than that corresponding to equal velocities of the rocket or airbreather (i.e., 6000 or 4000 feet per second) for this example, the rocket could be the preferred propulsion system for a tactical missile, the argument being that the mean velocity would be greater, hence the time-to-target would be less for the rocket. This in turn could perhaps permit more time for assessment prior to firing or time for more salvos in a shoot-look-shoot scenario.

The optimum cruise altitude for the rocket, assuming $C_L = L/q_0 A_R \approx 1$ at $(L/D)_{max}$, where $A_R = \pi D^2/4$, would be about 111,000 feet at u = 6000 feet per second and 93,000 feet at u = 4000 feet per second. Maximum range, however, occurs at lower altitudes because cruise range for the coasting rocket is small compared to the ranges of the optimal paths to points c. For the airbreathers, the corresponding altitudes for flying at $(L/D)_{max}$ would be 2000 to 4000 feet lower at the same velocity, but better performance would be achieved at slightly lower altitudes due to the aforementioned problems of low inlet and combustor efficiency at low pressure levels. Thus the cruise phase of the airbreather occurs at a somewhat lower angle of attack than that which yields $(L/D)_{max}$. For this example, optimum cruise altitude is about 95,000 feet for u = 6000 feet per second and 80,000 feet for u = 4000 feet per second.

The mission postulated in Fig. 13 is typical of a tactical missile that provides for its own guidance during the cruise phase and is, in fact, a long-range weapon. Thus, in the parlance currently in vogue, the performance shown in Fig. 14 is typical of a "wide area defense" missile, whereas that shown in Fig. 12 is typical of an "area defense" missile.

DESIGN PROCEDURES FOR AN AIRBREATHING MISSILE

Even though the details of the procedures used to design and develop an airbreathing missile cannot be covered, the overall approach can be outlined. Figure 15 is a flow chart showing this procedure. Initially, engine performance is determined using assumed efficiencies for the engine components, weights, and aerodynamics based on preliminary composite designs and constraints imposed by the guidance system, ordnance, stowage, etc. Parametric variations

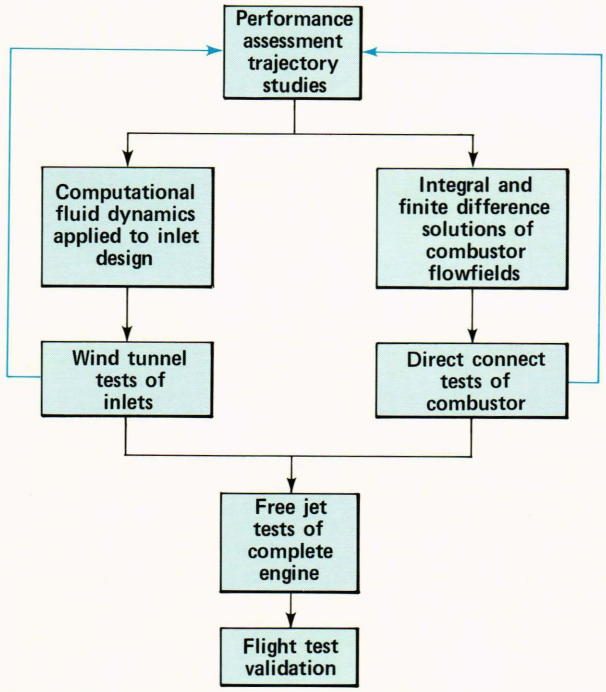

Figure 15 — Flow diagram for the design and development of a ramjet-powered missile.

are made in each of the above categories, and trajectories are flown to determine which candidate engine concepts can perform the proposed mission. Based on these results, computational techniques are used to obtain preliminary designs for candidate inlet configurations. Wind tunnel tests of inlets are made to provide revised performance values. A similar procedure is used in the development of the combustor. One or more iterations is made before a principal candidate engine geometry is chosen for verification in a free jet. The fuel supply and control system design is carried out concurrently with the inlet and combustor development and generally is used in the free-jet engine test. If all goes well, the engine then undergoes a flight test validation. A cursory examination of each of these steps follows.

Figure 16 shows results from one of the steps that take place in sizing the inlet and nozzle throat. Parametric variations of the inlet area A_i and the nozzle throat area A^* at various flight conditions and fuel flow rates are made to determine the thrust level. For a given fuel flow rate there exists a combination of A_i and A^* that yields the maximum thrust. For a subsonic combustion engine, this optimum occurs when the normal shock in the inlet compression process is located at the cowl lip station, as shown in the engine sketches. The solid curve is drawn through the locus of points corresponding to these optimal geometries. The curve terminates at the point where the maximum allowable A^* and the fuel/air equivalence ratio equals 1. This curve gives the performance of a variable geometry engine.

Taking the A_i and A^* that correspond to any point on the curve, e.g., point A, permits comparison of

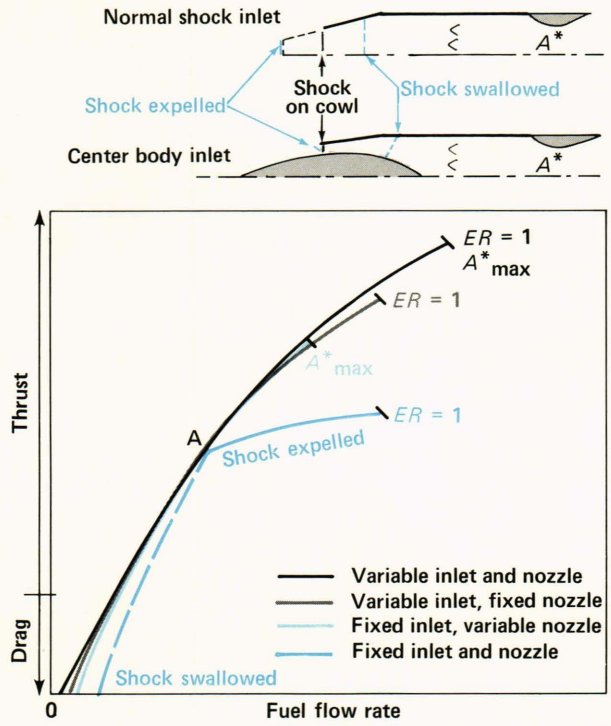

Figure 16 — The procedure used to determine inlet and nozzle throat dimensions.

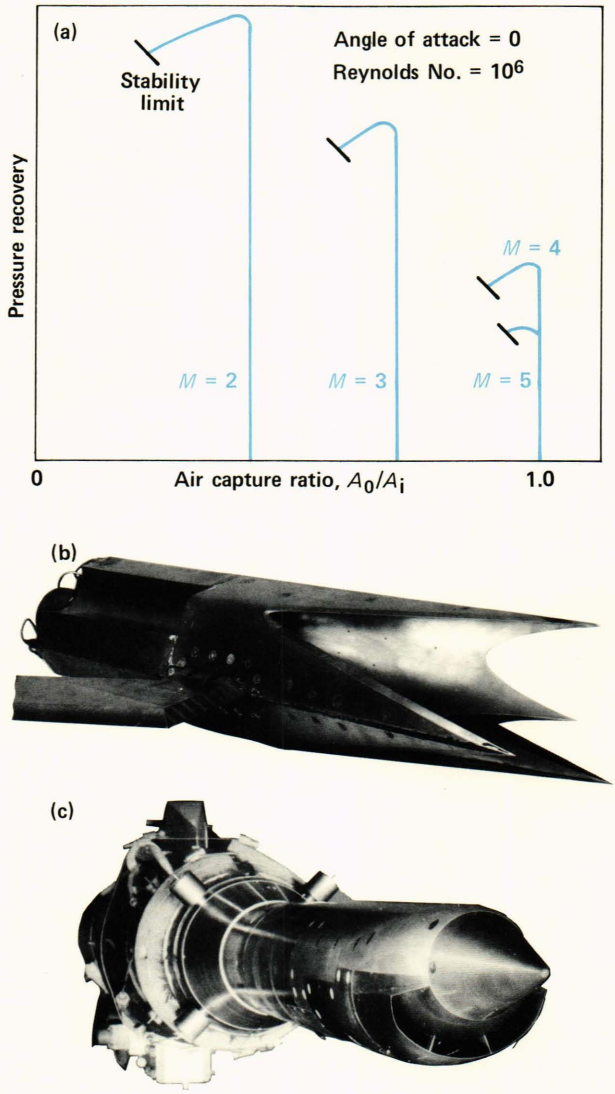

Figure 17 — Inlet testing. (a) Typical air capture-pressure recovery characteristics of an airbreathing missile inlet. (b) Three-module inlet evaluated in seven wind tunnel tests at M_0 = 4.0, 5.3, 6.0, 7.8, 8.1, and 10.0. (c) "Chin" type inlet model for a subsonic combustion ramjet tested at M_0 = 3.0 to 4.5.

partially variable and fixed geometry engines. If only the inlet can be varied, optimum performance is obtained with the shock on the cowl lip, but more fuel is required to produce the same thrust, and an equivalence ratio equal to 1 occurs at a lower thrust level. Likewise, with a fixed inlet and a variable exit, the normal shock is on the cowl lip, more fuel is required than for the variable geometry engine, and the maximum thrust is lower. With a fixed inlet and exit, the normal shock will be located on the cowl lip only at point a. For lower fuel rates, this shock is swallowed, as shown in the sketches, and the performance is correspondingly degraded. For higher fuel flow rates, the normal shock must be expelled, which may or may not be acceptable. In normal shock inlets that are used at relatively low flight speeds (i.e., less than Mach 2.2), no problems are encountered but, as shown in Fig. 16, the gains in thrust accrue only with large increases in fuel flow rates. With centerbody inlets that are used at higher speeds, expelling the shock much beyond the cowl lip generally results in the generation of an unacceptable instability sometimes referred to as "buzz." In a buzz condition, the airflow into the ramjet pulsates with a frequency equal to the fundamental or to a harmonic of the equivalent Helmholtz resonator.

The choice of point A in this discussion was arbitrary, and if more thrust were needed in a fixed geometry engine, a larger inlet would be dictated, albeit with an increased fuel flow and less efficiency at lower thrust levels.

INLET TESTING

Typical inlet testing is illustrated in Fig. 17. The flowfield of an inlet in flight can be simulated in a wind tunnel test as long as the Mach number and Reynolds number [(velocity·diameter)/kinematic viscosity] are duplicated. If the tests are performed at pressures higher than in flight or at temperatures lower than flight or both, the ratio ud/ν can be several times larger, and the diameter can thus be smaller. Typically, wind tunnel tests are carried out at one-fifth to one-third of the flight size. Tests are run over the entire range of Mach numbers and Reynolds numbers at all angles of attack expected in flight. For asymmetric designs, various roll orientations must also be examined.

The principal parameters that are measured in the test are pressure recovery, air capture, and cowl and additive drag. The details of both the internal and external flowfields and the inlet starting characteristics may also be of interest, especially if boundary layer separations or large gradients in the internal flow are present or if problems are expected in starting the engine. In Fig. 17a, pressure recovery as a function of air capture ratio A_0/A_i is shown for Mach 2 through 5 for a centerbody inlet designed for full capture at $M = M_D = 4$, angle of attack = 0 (M_D is the design Mach number). These data are obtained by closing a calibrated throttle attached to the inlet, which simulates the pressure rise that would be caused if combustion were present. As the throttle closes, the normal shock moves toward the cowl lip and the pressure recovery increases. When the normal shock passes upstream of the cowl, air capture decreases; with further closing of the throttle, the inlet reaches the aforementioned stability limit. The ratio of the cross-sectional area of the streamtube captured by the inlet to A_i is 1 for $M \geq M_D$. Pressure recovery corresponding to normal shock at the cowl lip increases with decreasing M.

Figures 17b and 17c are photographs of inlets tested for the Naval Sea Systems Command by APL. The three-module engine shown in Fig. 17b was tested in conjunction with the development of the engine shown in Fig. 3. Tests were made over a range of Mach numbers of 4 to 10 at angles of attack up to 15°. Figure 17c is a chin inlet that has been tested at $M = 2$ to 3.5.

COMBUSTOR DEVELOPMENT

Combustor development involves the direct-connect testing of the combustor chamber to an air ducting system that provides air at conditions simulating those provided by the inlet in flight. Since there is no unique similarity parameter for combustion, the tests must be made in full-scale hardware. In the course of the development of the combustor, numerous fuel injector and flame holder geometries are investigated. Other parameters that may be studied include the nozzle throat area, combustor length, port-to-dump area ratio in sudden expansion burners, and the effects of swirl. The standard measures of performance are combustion efficiency η_c and total (stagnation) pressure loss. The former is the ratio of the heat release actually realized to what is theoretically available in the fuel. The latter is a measure of all of the nonkinetic losses that are present.

Typical direct-connect testing data are shown in Fig. 18. Combustion efficiency varies with equivalence ratio, air total temperature, and pressure or weight flow. Both rich and lean blowout limits can be present, and regions where the combustion is unstable are often encountered. These instabilities can be either longitudinal or transverse. The former, relatively low frequency oscillations, can cause unfavorable interactions with the inlet; the latter, relatively high frequency oscillations, can produce detrimental effects on insulation materials, electronics components, etc.

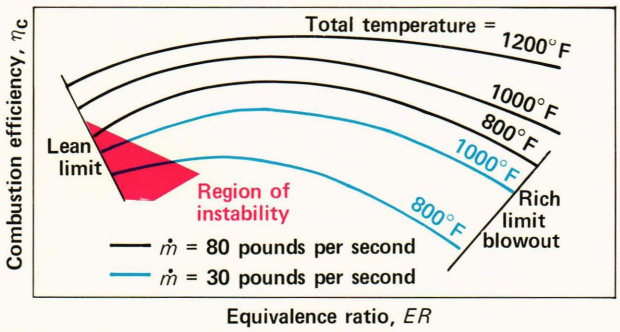

Figure 18 — The effects of temperature, pressure, and equivalence ratio on combustion efficiency in direct-connect testing of the combustion chamber.

Finally, in free-jet testing, the entire engine is placed in a large ground test facility. It is installed on a thrust stand to measure the net force on the engine. The entire test chamber is enclosed so that tests can be made that simulate high-altitude flight. Figure 19a shows an integral rocket ramjet that was tested in the free-jet facility at the Airbreathing Propulsion Test Unit at the Arnold Engineering Development Center, Tenn. Figure 19b shows typical test data. Successful completion of the free-jet engine tests provides the opportunity to proceed into a flight test program with reduced risk.

The development of other types of propulsion systems follows a similar approach to that diagrammed in Fig. 15, but the steps may differ depending on the components that must be tested. For example, rocket motor development obviously does not require inlet testing, but frequently attention must be given to tailoring the propellant composition to meet specific flight requirements. Because the coefficient a and exponent n in Eq. 4 are only weakly dependent on scale, most of the combustion characteristics of propellants can be obtained in a small-scale apparatus. Then, when a candidate fuel has been selected, full-scale motor firings are made to verify the small-scale results and to examine behaviors such as combustion instability that are scale dependent.

Much of the emphasis in the full-scale tests of rocket motors, and indeed in the testing of other propulsion cycles, addresses issues other than propulsion *per se,* e.g., the structural integrity of the propellant, rocket motor case, and nozzle. When the nozzle must provide thrust vector control, the operating characteristics of the actuating system, the structural adequacy of the gimbal or vanes, and the determination of the thrust degradation as a function of the lateral force generated must be examined.

The development of integral rocket ramjets requires not only all of the steps for both the rocket and the ramjet individually, but also a ground test demonstration of the transition from operation as a rocket to that as a ramjet. Even for cycles of this

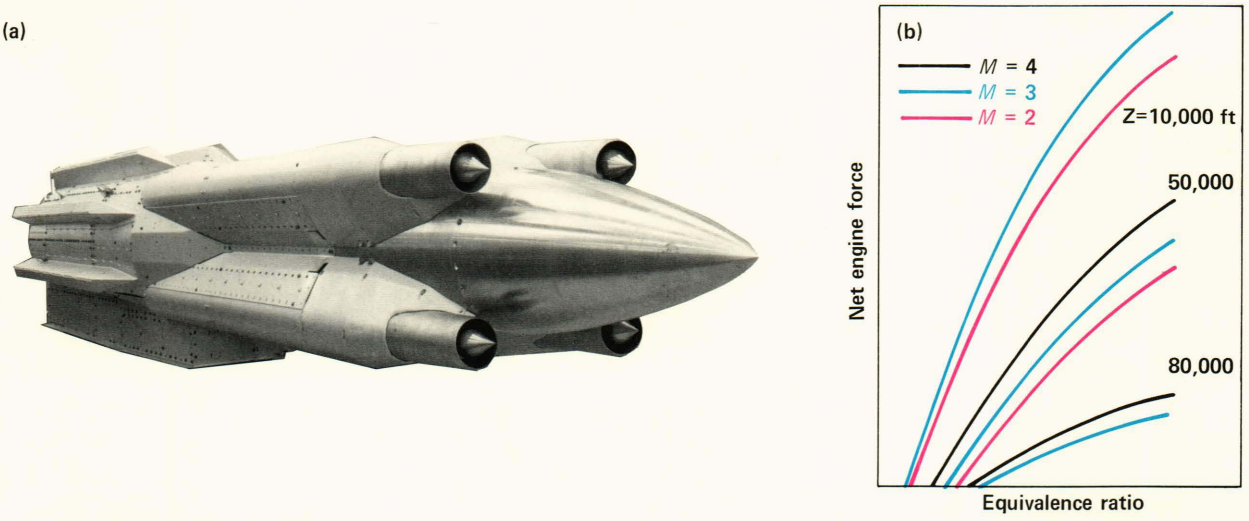

Figure 19 — Free jet engine testing. (a) Photograph of an integral rocket ramjet surface-to-surface engine with test fairings prior to testing in the Arnold Engineering Test Center free jet. (b) Typical measurements of engine force at various fuel flow rates and altitudes.

complexity, experience has shown that when meticulous attention is given to the resolution of all problems encountered in ground tests, near-flawless performance in flight test programs can be expected, as exemplified by the recently completed tests of the Advanced Strategic Air-Launched Missile for the United States Air Force.[5]

REFERENCES

[1] A. E. Bryson, Jr., and Y. C. Ho, *Applied Optimal Control*, Halsted Press, Washington, D.C. (1975).
[2] A. Miele, "Recent Advances in Gradient Algorithms for Optimal Control Problems," *J. Optimization Theory Appl.* **17**, 361-430 (Dec 1975).
[3] P. G. Hill and C. R. Peterson, *Mechanics and Thermodynamics of Propulsion,* Addison-Wesley, Reading, Mass. (1965).
[4] P. J. Waltrup, F. S. Billig, and R. D. Stockbridge, "Engine Sizing and Integration Requirements for Hypersonic Missile Applications," *NATO/AGARD/PEP 58th Symp. Conf. Proc. No. 307* (Oct 1981).
[5] J. Cushman, "Ramjet? Roger, Says DeLauer," *Defense Week,* 6-7 (Sep 27, 1982).